European Conference on Computational Fluid Dynamics
ECCOMAS CFD 2006
P. Wesseling, E. Oñate and J. Périaux (Eds)

VERIFICATION OF TURBULENCE MODELS WITH A MANUFACTURED SOLUTION

Eça L.[⋆]**, Hoekstra M.**[†]

[⋆]Department of Mechanical Engineering
Av. Rovisco Pais 1, 1049-001 Lisboa, Instituto Superior Técnico, Portugal
e-mail: eca@marine.ist.utl.pt

[†] R&D Department
P.O. Box 28, 6700 AA Wageningen, Maritime Research Institute Netherlands, The Netherlands
e-mail: M.Hoekstra@marin.nl

Key words: Code Verification, Manufactured solutions, Order of Accuracy, Turbulent Flow, Eddy-Viscosity

Abstract. *This paper presents an exercise of Code Verification with two manufactured solutions valid for 2D RANS equations supplemented either with the one-equation Spalart & Allmaras or with the two-equation BSL $k-\omega$ turbulence model. When the manufactured solution is applied with the eddy viscosity frozen, second order convergence behaviour is shown. When the solution of the eddy viscosity is included, the discretization of the turbulence quantities transport equations appear to influence the accuracy of the mean flow solution. The results show that a first-order accurate solution of the turbulence quantities transport equations may lead to first-order accurate solutions for the mean flow variables, even if the discretization of the continuity and momentum equations is second-order accurate. It also turns out that flux limiters can have an unfavourable effect on the convergence of the results with refinement of the grid.*

1 INTRODUCTION

The rapidly expanding capacity of Computational Fluid Dynamics (CFD) and the increase of its use in practical applications created the need to establish the credibility of the numerical results. This motivated an on-going debate about Verification & Validation in several forums, like the AIAA,[1] ERCOFTAC[2] or the ITTC.[3] At present, it is commonly accepted that the first step of this process is Code Verification.[4]

Code Verification intends to verify that a given code solves correctly the equations of the model by error evaluation.[4] Therefore, it requires a known solution to allow the determination of the error. The verifying process should demonstrate that the error tends to zero with grid refinement and that the observed order of accuracy matches the theoretical order of the discretization techniques used in the code.

The Reynolds-Averaged Navier-Stokes (RANS) equations have no analytical solutions and so to perform code verification in RANS solvers one has almost inevitably to apply the Method of the Manufactured Solutions[4–10] (MMS). Recently, manufactured solutions (MS) have been proposed[11,12] for wall-bounded turbulent flows including analytical functions for several one and two-equation eddy-viscosity turbulence models. The first results reported[12] for these MS's show that it is not trivial to set up a MS for the turbulence quantities of eddy-viscosity turbulence models. However, it is clear that the turbulence quantities transport equations must be included in the code verification process of RANS solvers based on eddy-viscosity models. One of the advantages of the MMS in RANS solvers is that one is able to compute the mean flow field with the manufactured eddy-viscosity or vice-versa. Therefore, it is possible to identify the source of any unexpected numerical behaviour of the solution.

In this paper, we have focused on the influence of the discretization techniques applied in the turbulence quantities transport equations on the convergence of the mean flow variables, i.e. the velocity components and the pressure. From the MS's[11,12] available, we have selected appropriate MS's for the Spalart & Allmaras[13] one-equation model and for the baseline (BSL) version of the $k-\omega$ two-equation model proposed by Menter.[14]

For the selected MS's, three different techniques were tested in the discretization of the convective terms of the turbulence quantities transport equations: first-order upwind discretization and third-order upwind discretization with and without flux limiters.[15]

These three alternatives were tested in the finite-difference[16] and finite-volume[15] 2-D versions of PARNASSOS. In order to evaluate the influence of accuracy of the determination of the eddy-viscosity on the mean flow variables, we have performed three types of exercises:

1. Calculate the mean flow field with the manufactured eddy-viscosity.
2. Calculate the eddy-viscosity with the manufactured velocity field.
3. Calculate the complete flow field.

The paper is organized in the following way: for the sake of completeness, section 2 presents the two MS's and section 3 contains a short description of the flow solver; the results are presented and discussed in section 4; finally, the conclusions are summarized in section 5.

2 MANUFACTURED SOLUTIONS

The computational domain is a square of side 0.5L with $0.5L \leq X \leq L$ and $0 \leq Y \leq 0.5L$ and the proposed Reynolds number, Rn, is 10^6.

$$Rn = \frac{U_1 L}{\nu} \ , \tag{1}$$

where U_1 is the reference velocity, L the reference length and ν the kinematic viscosity. In non-dimensional variables, (x, y), the computational domain is given by $0.5 \leq x \leq 1$ and $0 \leq y \leq 0.5$, where x stands for the horizontal direction and y for the vertical direction.

The main flow variables are identical for the two turbulence models. The velocity components in the x direction, u_x, and y direction u_y are given by

$$u_x = \mathrm{erf}(\eta) \quad \text{and} \quad u_y = \frac{1}{\sigma\sqrt{\pi}}\left(1 - e^{-\eta^2}\right) \ . \tag{2}$$

η is a "similarity variable"

$$\eta = \frac{\sigma y}{x} \ , \tag{3}$$

where is $\sigma = 4$.

The pressure coefficient (i.e. the pressure relative to twice the reference dynamic pressure) is given by

$$C_p = \frac{P}{\rho(U_1)^2} = 0.5\ln\left(2x - x^2 + 0.25\right)\ln\left(4y^3 - 3y^2 + 1.25\right) \tag{4}$$

2.1 Spalart & Allmaras one-equation model

In the Spalart & Allmaras[13] one-equation model the eddy-viscosity, ν_t, is given by

$$\nu_t = \tilde{\nu} f_{v1} \tag{5}$$

with

$$f_{v1} = \frac{\chi^3}{\chi^3 + c_{v1}^3} \ , \ \chi = \frac{\tilde{\nu}}{\nu} \quad \text{and} \quad c_{v1} = 7.1 \ . \tag{6}$$

As discussed by Eça & Hoekstra,[11] a MS for the Spalart & Allmaras model should preferably specify the dependent variable of the model, $\tilde{\nu}$. If instead the eddy-viscosity, ν, is specified, the non-linearity of the damping function f_{v1} causes serious trouble. In the selected MS,[12] designated here by MS2, $\tilde{\nu}$ is given by

$$\tilde{\nu} = \tilde{\nu}_{max}\eta_\nu^2 e^{1-\eta_\nu^2} \ , \tag{7}$$

where

$$\eta_\nu = \frac{\sigma_\nu y}{x} \ , \tag{8}$$

$\sigma_\nu = 2.5\sigma$ and $\tilde{\nu}_{max}$ is $10^3\nu$.

2.2 BSL $k-\omega$ two-equation model

In the two-equation BSL $k-\omega$ turbulence model the eddy-viscosity is given by

$$\nu_t = \frac{k}{\omega} \tag{9}$$

In the selected MS,[11] analytical expressions are provided for ν_t and k. The ω field is derived from equation (9). What we will call here the MS4 solution specifies the following equations for ν_t, k and ω:

$$\nu_t = 0.25(\nu_t)_{max}\eta_\nu^4 e^{2-\eta_\nu^2} \ , \tag{10}$$

$$k = k_{max}\eta_\nu^2 e^{1-\eta_\nu^2} \ , \tag{11}$$

$$\omega = 4\frac{k_{max}}{\nu_{max}} e^{-1}\eta_\nu^{-2} \ , \tag{12}$$

where $(\nu_t)_{max} = \tilde{\nu}_{max} = 10^3\nu$.

The BSL model includes a blending function, F_1, which does not have well-defined derivatives in the complete flow field, as discussed in Eça *et al.*[11] Therefore, for code verification purposes, the dependency of the constants σ_k and σ_ω on F_1 has been removed: $\sigma_k = \sigma_\omega = 2$.

3 FLOW SOLVER

The calculations were performed with the 2-D finite-difference[16] (FD) and finite-volume[15] (FV) versions of PARNASSOS. Both versions solve the steady, incompressible, RANS equations without any transformation of the continuity equation. The main properties of the two versions are summarized below:

- The finite-difference, FD, version discretizes the continuity and momentum equations written in Contravariant form, which is a weak conservation form. The finite-volume, FV, version discretizes the strong conservation form of the equations.

- The FD version computes the momentum balance along the directions of the curvilinear coordinate system, whereas the FV version calculates the momentum balance for its Cartesian components.

- The FD code has a fully-collocated arrangement with the unknowns and the discretization centered at the grid nodes. In the FV code unknowns are defined at the centre of each cell.

- Both versions of the code include two layers of virtual grid nodes at each boundary of the computational domain. These virtual grid nodes guarantee that the stencil of the third-order schemes can be kept in the vicinity of the boundaries of the domain.

- Both versions apply Newton linearization to the convective terms and are at least second order accurate for all the terms of the continuity and momentum equations. Third-order upwind discretization is applied to the convective terms.
- The linear system of equations formed by the discretized continuity and momentum equations is in both versions solved simultaneously with GMRES[17] using a coupled ILU preconditioning.
- The solution of the turbulence quantities transport equations is uncoupled from solving the continuity and momentum equations.

In both versions, we have tested three alternative discretizations of the convective terms of the turbulence quantities transport equations:

- First-order upwind discretization, O1.
- Third-order upwind discretization, O3.
- Third-order upwind discretization with flux limiters,[15] LIM.

The use of flux limiters (to avoid non-physical oscillatory solutions) is common practice in CFD, but its influence on the convergence properties of the code remains obscure. Basically, the flux limiters tested in this work blend the first and third-order discretizations according to the local variation of the dependent variable. As discussed by Knupp & Salari,[9] this may have consequences for the convergence properties of all the flow variables. Flux limiting thus deserves attention in this paper.

4 RESULTS

Although in some cases we have tested more than one grid set,[18] in this paper we will focus on the results obtained in a single set of Cartesian grids. These grids have equidistant grid node distributions in the x direction, but in the y direction the grid is clustered towards the bottom boundary using a one-sided stretching function,[19] (stretching parameter 0.05).

The grid set includes 16 geometrically similar grids covering a grid refinement ratio of 4. The finest grid has 401×401 grid nodes and the coarsest grid 101×101. There are 19×19 physical locations which are common to all grids. In the FD approach, this allows the determination of the convergence properties of local flow quantities without interpolation.

4.1 Monitoring the Error

Following Roache,[4] the error of any flow quantity, ϕ, can be expressed by a power series expansion. Retaining only the lowest order term, we have

$$e(\phi) = \phi - \phi_{ms} \simeq \alpha h_i^p \ , \tag{13}$$

where the subscript $_{ms}$ identifies the manufactured solution, α is a constant, h_i is the typical cell size and p is the order of accuracy.

For the present grids,

$$h_i = \frac{1}{NX} = \frac{1}{NY} \ .$$

NX and NY stand for the number of nodes in the x and y directions.

We have quantified the error in the numerical solution by monitoring both local (for the FD approach) and global (e.g. friction force on bottom wall) quantities.[18] However,in the present paper we will restrict ourselves to the global quantities.

For a given flow quantity, ϕ, we have computed the Root Mean Square (RMS) of the error of the numerical solution, which is given by:

$$RMS(e(\phi)) = \sqrt{\sum_{i=2}^{NX-1} \sum_{j=2}^{NY-1} \frac{(\phi(j,i) - \phi(j,i)_{ms})^2}{(NX-2)(NY-2)}} \ . \tag{14}$$

i is the index of the node in the x direction and j is the index of the node in the y direction.

In the results presented in the remainder of this section, the observed order of accuracy, p, and the constant α are determined with a least squares root approach.[20] The fits plotted in the figures are obtained with the data of the 11 finest grids of each set, i.e. the grids with at least 201×201 grid nodes, covering a grid refinement ratio of 2. However, we have also checked the dependence of the observed order of accuracy on the selected grids. The observed order of accuracy is estimated for different groups of grids, which must present a grid refinement ratio between the finest and coarsest grid, $r_{i1} = h_i/h_1$, of at least 1.3. This is an important check, because it indicates whether the data obtained in the finest grids are in the so-called ‘asymptotic range’.

In all the calculations presented below the iterative error was reduced to machine accuracy and the calculations were performed with 15-digits precision. Therefore, the computed errors are mainly a consequence of the discretization error.

4.2 Calculation of the Flow Field with the Manufactured Eddy-viscosity

The first exercise performed was the calculation of the pressure and velocity fields with the eddy-viscosity taken from the MS2 and MS4. In both versions of the code, the MS was used as a "turbulence model", i.e. the MS was used to determine ν_t at the nodes (FD) or at the cell centre (FV).

The MS enables the choice of several types of boundary conditions. The present option intends to reproduce the type of conditions applied in a near-wall turbulent flow. The subscript $_{ms}$ identifies the MS solution. The boundary conditions applied to the horizontal velocity component, u_x, vertical velocity component, u_y, and the pressure coefficient, C_p, are:

- Bottom boundary, $y = 0$:

$$u_x = (u_x)_{ms} = 0 \ , \quad u_y = (u_y)_{ms} = 0 \ .$$

- Inlet boundary, $x = 0.5$:

$$u_x = (u_x)_{ms} \ , \quad u_y = (u_y)_{ms} \ .$$

- Top boundary, $y = 0.5$:

$$u_x = (u_x)_{ms} \ , \quad C_p = (C_p)_{ms} = 0 \ .$$

- Outlet boundary, $x = 1.$:

$$\frac{\partial u_x}{\partial x} = \left(\frac{\partial u_x}{\partial x}\right)_{ms} \ , \quad \frac{\partial u_y}{\partial x} = \left(\frac{\partial u_y}{\partial x}\right)_{ms} \quad C_p = (C_p)_{ms} \ .$$

The "numerical" boundary conditions required for u_y at the top boundary and C_p at the inlet and bottom boundaries were imposed using the first or second derivatives available from the MS. In the present calculations, the virtual layers were filled-in numerically, i.e. the dependent variables at the virtual nodes were not defined from the MS.

Figure 1 presents the convergence of the RMS of u_x, u_y and C_p for the MS2 and MS4 with the two versions of the code. The plots include also the convergence of the friction resistance at the bottom, C_D. The results exhibit the theoretical order of accuracy for all the flow variables, $p = 2.0$, and the data are clearly in the so-called "asymptotic range".

4.3 Calculation of the Eddy-Viscosity with the Manufactured Velocity Field

The second test is to solve the transport equations for the turbulence quantities to determine the eddy-viscosity with the manufactured velocity field.

In the calculations with the FD code, Dirichlet boundary conditions were applied at the four boundaries of the computational domain for all the turbulence quantities. With the MS, this is straightforward for the dependent variable of the one-equation model, $\tilde{\nu}$ and the turbulence kinetic energy, k. However, ω, goes to infinity at the bottom of the computational domain, analogous to what happens in solving a physical flow problem. In

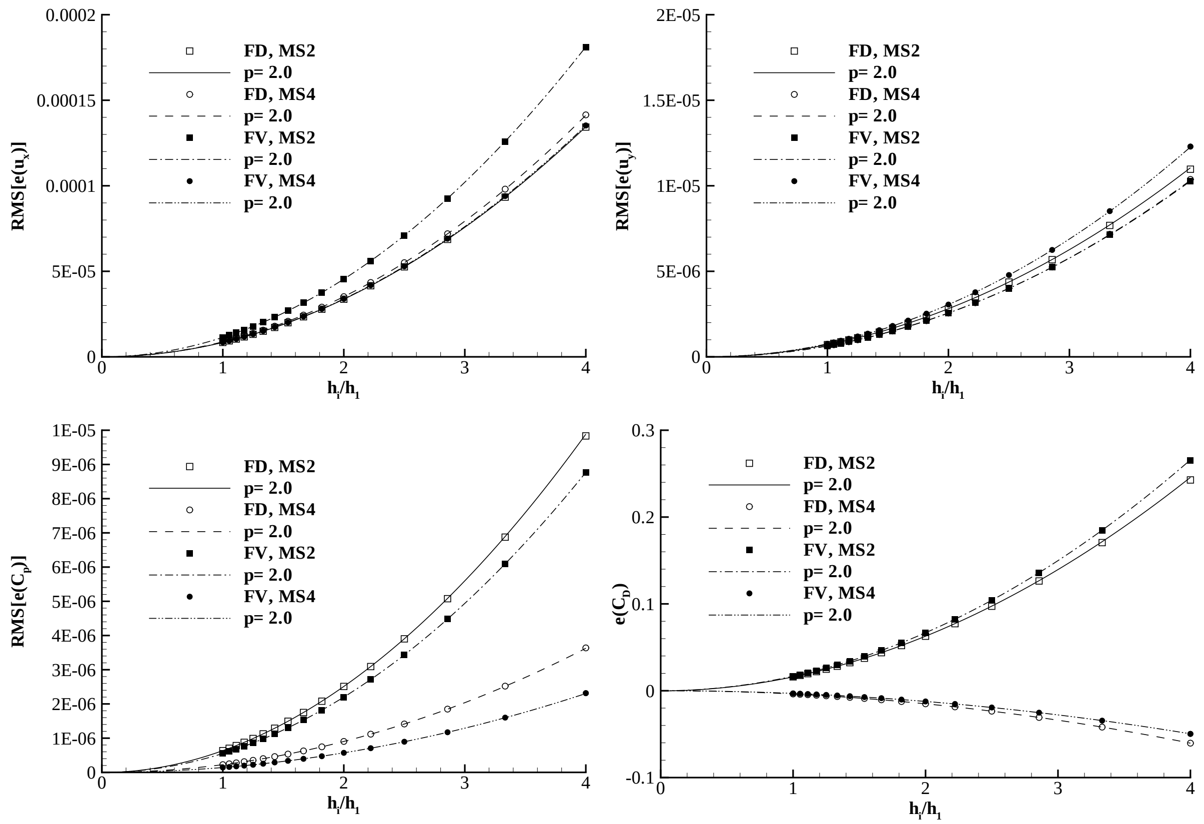

Figure 1: Convergence of the RMS of u_x, u_y and C_p and the friction resistance coefficient at the bottom, C_D, with the grid refinement. Velocity and pressure fields calculated with the manufactured eddy-viscosity field.

order to avoid any influence of the boundary value of ω, we have fixed ω at the first two layers of grid nodes away from the bottom ($j = 2$ and $j = 3$) using the MS.

With the FV code, we have only performed calculations for the Spalart & Allmaras model using Dirichlet boundary conditions at the inlet, bottom and top boundaries. Neumann boundary conditions were imposed at the outlet, with the first derivative of $\tilde{\nu}$ with respect to x taken from the MS.

For both versions of the code, we have performed calculations with three alternative discretizations of the convective terms of the turbulence quantities transport equations: first-order upwind, O1; third-order upwind, O3 and third-order upwind with limiters, LIM.

Figure 2 presents the convergence of the eddy-viscosity, ν_t, with the O1, O3 and LIM approaches. The data show several interesting features:

- The observed order of accuracy is close to the expected values: 1 for the O1 approach and 2 for the O3 option. Moreover, the value of p is hardly influenced by the choice of the group of grids used to determine p.

- The error constant, α, is one order of magnitude larger for the first-order discretization than for the third-order approach.

- The use of limiters makes the theoretical order of the method grid dependent. The results with limiters exhibit an error level close to the third-order data. However, with the increase of the grid refinement, the percentage of locations with active limiters increases (specially for the FD code) which causes the observed deviation from the second-order convergence. In these cases, it is impossible to perform a reliable Richardson extrapolation.

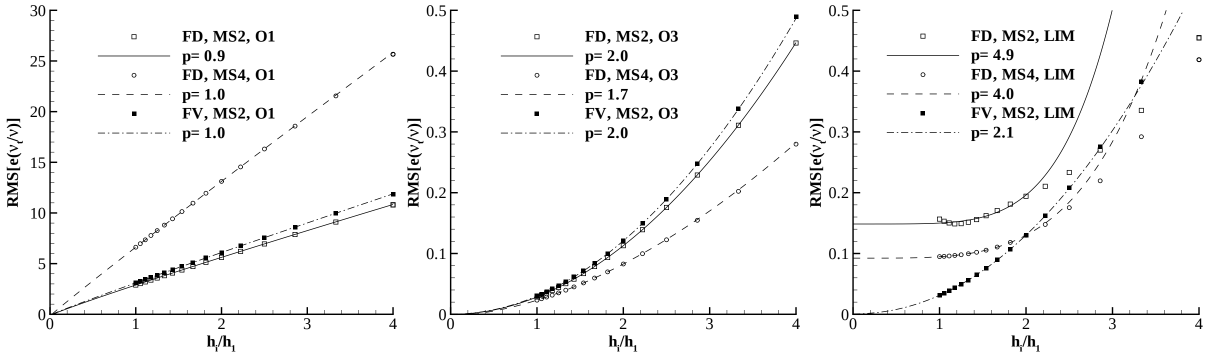

Figure 2: Convergence of the RMS of ν_t with grid refinement. Eddy-viscosity calculated with the manufactured velocity field. MS2≡ Spalart & Allmaras one-equation model. MS4≡ BSL $k-\omega$ two-equation model.

4.4 Calculation of the complete flow field

The third exercise is the calculation of the complete flow field. The boundary conditions are equivalent to the ones described above for the previous exercises. In this case, we have applied Neumann boundary conditions at the outlet for all the turbulence quantities.

The calculation of the MS2 with the Spalart & Allmaras turbulence model is troublesome.[12] With the O1 and LIM options, we were not able to obtain converged solutions with either version of the code. The problem is related to the appearance of negative turbulence quantities, which are not accepted in both versions of the code. Therefore, for the MS2 with the Spalart & Allmaras turbulence model we present only results with the O3 approach.

Figure 3 presents the RMS of the error of u_x, u_y, C_p and ν_t as a function of the grid refinement for the MS2. We observe that:

- Only in exceptional cases does the RMS of the selected flow variables exhibit the theoretical order of accuracy. Furthermore, the value of p varies with the group

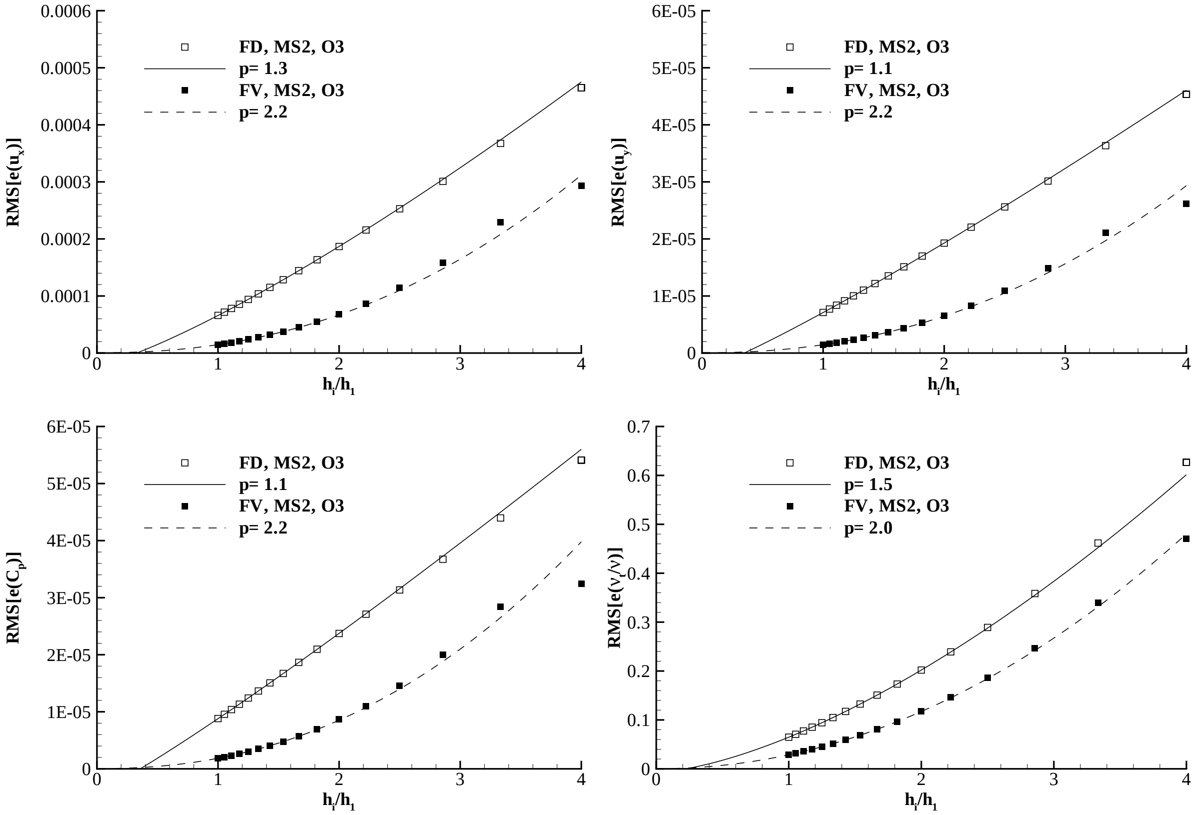

Figure 3: Convergence of the RMS of u_x, u_y, C_p and ν_t with the grid refinement. MS2 with the Spalart & Allmaras one-equation turbulence model.

of grids selected for its determination. Therefore, the data are not in the so-called 'asymptotic range'.

- Unlike what was seen in the two previous exercises, the convergence of the two versions of the code is not similar:
  - In both codes, the error constant, α, is larger than the value obtained in the previous exercises for the four flow variables.
  - Surprisingly, the eddy-viscosity exhibits the values of p closest to the theoretical order of the method in both versions of the code.
  - In the FD version, p is below 2 for the selected flow variables but it tends to increase with grid refinement.
  - On the other hand, the FV version leads to p above 2 while p decreases with the grid refinement.

The different behaviour of the two versions of the code is linked to the way in which the $\tilde{\nu}$ transport equation is written. In the Spalart & Allmaras model,[13] there is a term proportional to the dot product of the gradient of $\tilde{\nu}$. In the FV version, this term is integrated on each cell in its original form, whereas the FD version discretizes an equivalent equation that transforms this dot product in two divergence type terms. Nevertheless, in both versions of the code we obtain the same trend: the convergence properties of the complete flow calculations are not equivalent to the ones obtained in the calculation of the velocity and pressure fields with the manufactured eddy-viscosity or in the calculation of the eddy-viscosity with the manufactured velocity field.

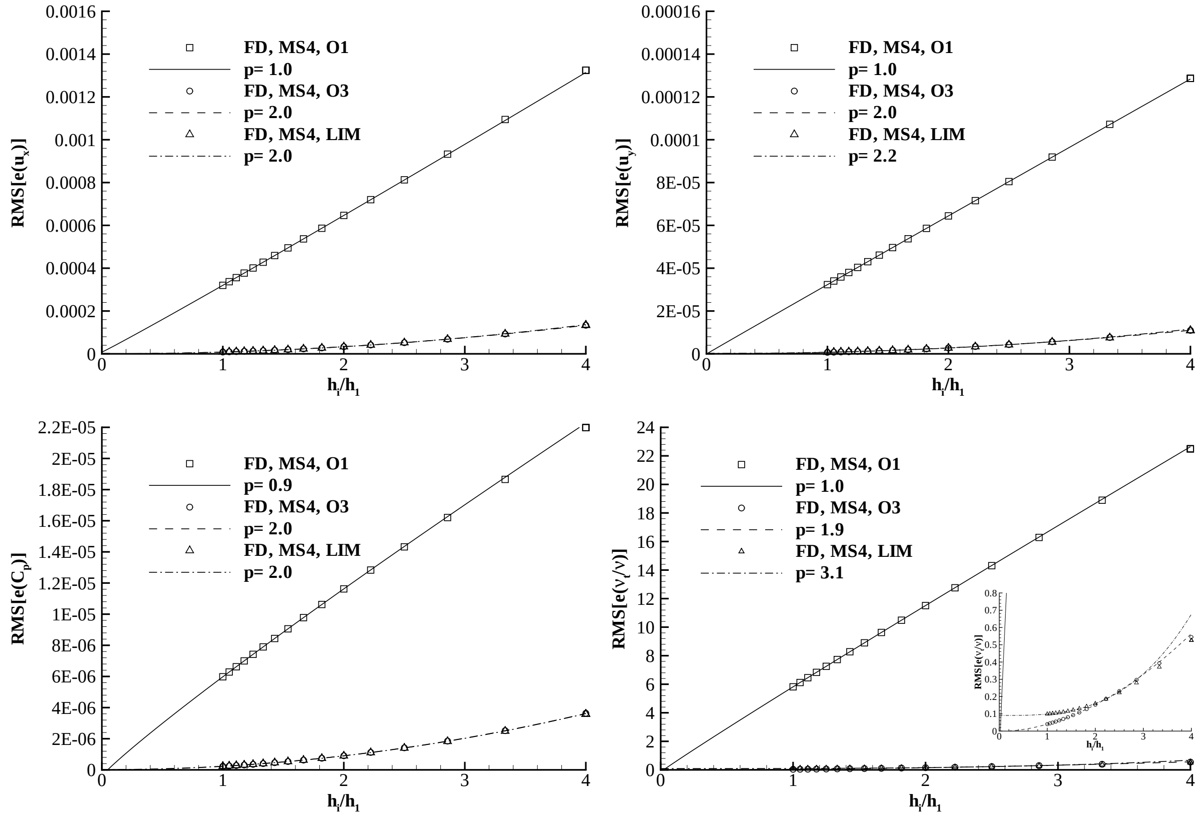

Figure 4: Convergence of the RMS of u_x, u_y, C_p and ν_t with the grid refinement. MS4 with the BSL $k-\omega$ model two-equation turbulence model.

Figure 4 shows the convergence of the RMS of u_x, u_y, C_p and ν_t with grid refinement for the MS4 with the BSL $k-\omega$ model. The plots include the solutions of the FD version with the O1, O3 and LIM approaches. Again, there are interesting trends in the data plotted in figure 4:

- The convergence of u_x, u_y and C_p is first-order accurate for the solutions obtained with the first-order discretization of the convective terms of the k and ω transport equations. On the other hand, the theoretical order of accuracy is observed for the O3 approach.

- The error constant, α, for u_x, u_y and C_p is substantially larger for the O1 approach than for the O3 option.
- As for the previous exercise, the effect of the limiters makes the code accuracy grid dependent. However, this effect is only observed for ν_t. u_x and C_p present the same convergence properties for the O3 and LIM options. Only u_y shows a small influence of the different convergence behaviour of ν_t.

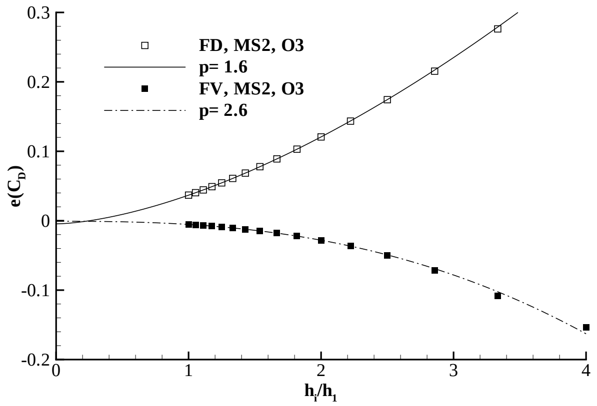

Figure 5: Convergence of the friction resistance at the bottom, C_D, with the grid refinement. MS2 with the Spalart & Allmaras one-equation model and MS4 with the BSL $k-\omega$ two-equation model.

The convergence of C_D for the MS2 and MS4 solutions with the grid refinement is depicted in figure 5. The results confirm the trends discussed above for the main flow variables. In the MS2, the observed order of accuracy is smaller than the theoretical value for the FD version, whereas the FV code exhibits p larger than 2.0. In both cases, p is dependent on the grids selected and it tends to 2.0 with the grid refinement. It is also interesting to remark that for the MS4 the solution with limiters exhibits the theoretical order of accuracy, $p = 2.0$, but a larger error constant than the solution without limiters.

5 CONCLUSIONS

The present paper presents a code verification exercise for two manufactured solutions appropriate for the Spalart & Allmaras one-equation model and for the BSL version of the $k-\omega$ two-equation model. Three types of exercises have been performed: calculation of the velocity field with the manufactured eddy-viscosity; calculation of the eddy-viscosity with the manufactured velocity field; calculation of the complete flow field.

The results show that it is important to include the turbulence model transport equations in the Code Verification process. In particular, the Spalart & Allmaras model exhibits different convergence properties when the velocity field is taken from the manufactured solution or is part of the calculation. Similarly, the convergence properties of the velocity and pressure fields with the manufactured eddy-viscosity are not equivalent to what is obtained with the simultaneous solution of the turbulence model transport equation.

Three discretization techniques were tested for the convective terms of the turbulence quantities transport equations: first-order upwind; third-order upwind and third-order upwind with flux limiters. Two main conclusions are drawn from the tests performed:

- A first-order accurate solution of the turbulence model transport equations may lead to a first-order accurate solution for the velocity and pressure fields.
- The use of flux limiters makes the order of accuracy of the code grid dependent. In the present test cases, the error of the solution with limiters is much closer to the third-order discretization than to the first-order approach. However, error estimates based on Richardson extrapolation do not work when the limiters are active.

The present paper illustrates the potential of the Method of the Manufactured Solutions for code verification in turbulent flows. Moreover, it also suggests that physical realistic solutions can be very useful for testing error estimation techniques.

REFERENCES

[1] Guide for the Verification and Validation of Computational Fluid Dynamics Simulations, AIAA-G077-1998.

[2] Best Practice Guidelines, Version 1.0, ERCOFTAC Special Interest Group on "Quality and Trust in Industrial CFD", January 2000.

[3] ITTC Quality Manual

[4] Roache P.J. - *Verification and Validation in Computational Science and Engineering* - Hermosa Publishers, 1998.

[5] Pelletier D., Roache P.J. - *CFD Code Verification and the Method of the Manufactured Solutions* - 10^{th} Annual Conference of the CFD Society of Canada, Windsor, Ontario, Canada, June 2002.

[6] Oberkampf W.L., Blottner F.G., Aeschliman D.P. - *Methodology for Computational Fluid Dynamics code Verification/Validation.* - AIAA 26^{th} Fluid Dynamics Conference, AIAA Paper 95-2226, San Diego, California, June 1995.

[7] Turgeon É., Pelletier D., - *Verification and Validation of Adaptive Finite Element Method for Impingement Heat Transfer* - Journal of Termophysics and Heat Transfer, Vol. 15, 2001, pp. 284-292.

[8] Turgeon É., Pelletier D., - *Verification and Validation in CFD using an Adaptive Finite Element Method* - Canadian Aeronautic and Space Journal, Vol. 48, 2002, pp. 219-231.

[9] Knupp P., Salari K. - *Verification of Computer Codes in Computational Science and Engineering* - CRC Press, 2002.

[10] Roache P.J. - *Code Verification by the Method of the Manufactured Solutions* - ASME Journal of Fluids Engineering, Vol. 114, March 2002, pp. 4-10.

[11] Eça L., Hoekstra M., Hay A., Pelletier D. - *A Manufactured Solution for a Two-Dimensional Steady Wall-Bounded Incompressible Turbulent Flow* - 7^{th} World Congress on Computational Mechanics, Los Angeles, July 2006.

[12] Eça L., Hoekstra M., Hay A., Pelletier D. - *On the Construction of Manufactured Solutions for One and Two-Equation Eddy-Viscosity Models* - 7^{th} World Congress on Computational Mechanics, Los Angeles, July 2006.

[13] Spalart P.R., Allmaras S.R. - *A One-Equations Turbulence Model for Aerodynamic Flows* - AIAA 30th Aerospace Sciences Meeting, Reno, January 1992.

[14] Menter F.R. - *Two-Equation Eddy-Viscosity Turbulence Models for Engineering Applications* - AIAA Journal, Vol.32, August 1994, pp. 1598-1605.

[15] Hoekstra M. - *Numerical Simulation of Ship Stern Flows with a Space-marching Navier-Stokes Method* - PhD Thesis, Delft 1999.

[16] José M.Q.B. Jacob, Eça L. - *2-D Incompressible Steady Flow Calculations with a Fully Coupled Method* - VI Congresso Nacional de Mecânica Aplicada e Computacional, Aveiro, April 2000

[17] Saad Y, Schultz M.H. - *GMRES: a generalized minumum residual algorithm for solving nonsymmetric linear systems* - SIAM Jnl. Sci. Statist. Comp., Vol. 7, pp 856-869, 1986.

[18] Eça L. - *Calculation of a Manufactured Solution for a 2-D Steady Incompressible Near-Wall Turbulent Flow with PARNASSOS* - IST Report D72-35, January 2006.

[19] Vinokur M. - *On One-Dimensional Stretching Functions for Finite-Difference Calculations.* - Journal of Computational Physics, Vol. 50, 1983, pp. 215-234.

[20] Eça L, Hoekstra M., *An Evaluation of Verification Procedures for CFD Applications*, 24^{th} Symposium on Naval Hydrodynamics, Fukuoka, Japan, July 2002.